REVIEW
SOLID EARTH

*Earth and Planetary Physics*
*2*: 173–188, 2018
doi: 10.26464/epp2018018

# Evidence supporting New Geophysics

**Stuart Crampin[1,2], and Yuan Gao[3]***

[1]British Geological Survey, The Lyell Centre, Edinburgh EH14 4AP, Scotland UK;

[2]School of GeoSciences, University of Edinburgh EH9 3FW, Scotland UK;

[3]Institute of Earthquake Forecasting, China Earthquake Administration, 100036 Beijing, China

**Abstract:** In the last decade a New Geophysics has been proposed, whereby the crust and uppermost ~400 km of the mantle of the Earth are so pervaded by closely-spaced stress-aligned microcracks (intergranular films of hydrated melt in the mantle) that *in situ* rocks verge on failure by fracturing, and hence are critical-systems that impose a range of fundamentally-new properties on conventional sub-critical geophysics. Enough of these new properties have been observed to confirm that New Geophysics is a new understanding of fluid/rock deformation with important implications and applications. Evidence supporting New Geophysics has been published in a wide variety of publications. Here, for clarification, we summarise in one document the evidence supporting New Geophysics.

**Keywords:** earthquakes; eruptions; microcracks; New Geophysics; shear-wave splitting; stress-forecasting

**Citation:** Crampin, S., and Gao, Y. (2018). Evidence supporting New Geophysics. *Earth Planet. Phys.*, *2*(3), 173–188. http://doi.org/10.26464/epp2018018

## 1. Introduction

Stress-aligned shear-wave splitting (SWS) (seismic birefringence) is widely observed: in the shear-wave window at the Earth's surface above small earthquakes in geological and tectonic regimes worldwide (Crampin, 1994; Gerst and Savage, 2004; Crampin and Peacock, 2008; Crampin and Gao Y, 2013; Gao Y et al., 1995, 2010, 2011; Shi YT et al., 2009; Zhao B et al., 2012); in record sections of seismic exploration (Alford, 1986; Angerer, 2002; Helbig and Thomsen, 2005); and in shear-waves propagating through the uppermost ~400 km of the mantle (Silver, 1996; Savage, 1999; Gao Y et al., 2010). The SWS in the mantle, although typically attributed to propagation through stress-aligned mantle crystals, is arguably more likely to be caused by stress-aligned intergranular films of hydrated melt (Crampin, 2003). (The shear-wave window discussed by Booth and Crampin (1985) is the range of ray path incident-angles at the free surface which are less than the critical angle for P-wave reflections, $\sin^{-1}(V_S/V_P)$, typically less than ~35°, for which incident shear-wave waveforms are preserved at surface observations.)

Indicative of some form of seismic anisotropy, in principle SWS could be caused by a variety of different phenomena. However, the only anisotropic symmetry system with the observed parallel SWS polarisations at a horizontal free-surface is hexagonal symmetry (transverse isotropy) with a horizontal axis of cylindrical symmetry (Crampin, 1981; Crampin and Kirkwood, 1981). This is commonly referred to as HTI-symmetry, and the only common geological phenomenon that has HTI-symmetry in almost all rocks is stress-aligned parallel vertically-oriented fluid-saturated microcracks (Crampin, 1994; Crampin and Peacock, 2008; Crampin and Gao Y, 2013; Gao Y et al., 1995). Seismic propagation in distributions of parallel vertically-orientated thin-layers would also have HTI-symmetry, but such distributions are rarely found. Consequently, observation of parallel SWS polarisations at the surface immediately indicates distributions of parallel vertical stress-aligned microcracks along shear-wave ray paths at depth within the Earth. Such SWS is illustrated schematically in Figure 1. Since microcrack geometry is sensitive to changes of stress and controls SWS (Crampin, 1994; Crampin and Peacock, 2008; Crampin and Gao Y, 2013; Gao Y and Crampin, 2004; Gao Y et al., 1998; Teanby et al., 2004; Gerst and Savage, 2004), observations of SWS provide the opportunity to monitor changes of stress deep within the Earth.

Note that occasionally the polarization of the observed SWS is orthogonal to the direction of maximum stress. This is typically when shear-wave ray paths penetrate the critically high-pressure envelopes enclosing all seismically-active fault planes. Such high-pressures induce 90°-flips (Angerer et al., 2002) into the polarizations of leading split shear-waves (Crampin et al., 2002, 2004a).

The degree of observed SWS in ostensibly unfractured rock throughout the crust and upper mantle is from a minimum of ~1.5% to a maximum of ~4.5% shear-wave velocity anisotropy (~1.5%SWVA to ~4.5%SWVA) (Crampin, 1994; Crampin and Peacock, 2008; Crampin and Gao Y, 2013). Crack density is a dimensionless parameter $\varepsilon \approx Na^3/v$, where $N$ is the number of cracks of radius $a$ in volume $v$ (Hudson, 1981). Since $\varepsilon$ is approximately %SWVA/100, the observed percentages of SWVA indicate crack-densities $\varepsilon \approx$ ~0.015 to ~0.045 as imaged in Figure 2 (Crampin, 1994), which shows cross-sections of uniform three-dimensional

Correspondence to: Y. Gao, qzgyseis@163.com
Received 12 MAR 2018; Accepted 25 APR 2018.
Accepted article online 14 MAY 2018.

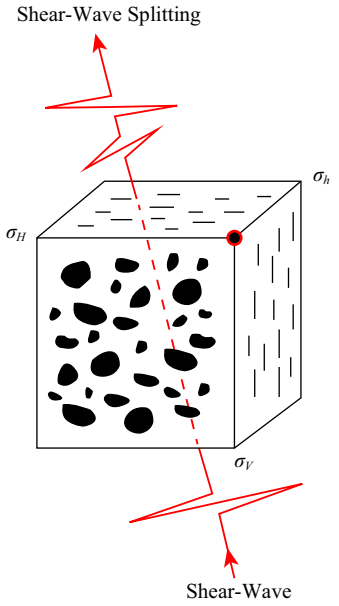


**Figure 1**. Schematic illustration of shear-wave splitting in stress-aligned microcracked rock, where $\sigma_H$, $\sigma_h$, and $\sigma_V$ are the maximum-horizontal, minimum-horizontal, and vertical stresses, respectively.

distributions of parallel vertical penny-shaped cracks for a range of values of SWVA. Although we do not suggest the microcracks are necessarily penny-shaped, the *in situ* microcracks are so small and so numerous that small deviations make negligible differences to SWS observations (Crampin, 1994; Crampin and Peacock, 2008; Crampin and Gao Y, 2013).

The first two images in Figure 2, for the observed SWVA ~1.5% to ~4.5%, show that 'microcracks' are so closely-spaced in the Earth that they verge on failure (at *fracture-criticality*) and hence are critical-systems (Davies, 1989a; Crampin and Peacock, 2005, 2008; Crampin and Gao Y, 2013). Fracture-criticality is the level of cracking at which rocks will fracture if there is any disturbance. The observed SWVA in Figure 2 shows that microcracks verge on fracture-criticality at SWVA just above 4.5%. We identify fracture-criticality with the percolation threshold, which for fluid-saturated stress-aligned microcracked rock is at $\varepsilon \approx$ ~0.05 (~5%SWVA) (Crampin and Zatsepin, 1997). The behaviour of phenomena verging on failure at singularities (aka double-points, tipping-points, bifurcations, or the case of geophysics, fracture-criticality) imposes a range of fundamentally-new properties on conventional sub-critical physics that are part of a *New Physics* (Davies, 1989b). Hence the proposed *New Geophysics* (Crampin, 2004, 2006), reviewed by Crampin and Gao Y (2013). For convenience, Supplementary Material briefly summarises New Geophysics and Table S1 lists some of the new properties imposed by the critically microcracked Earth.

New Geophysics is a fundamental revision of conventional sub-critical geophysics and, like all such fundamental revisions, particularly concerning criticality, tends to be controversial –see the exchanges of views between Crampin (2011, 2012) and Jordan and Jones (2011) and Jordan et al. (2012). Evidence and support for New Geophysics has been published in some dozen papers in different journals, which has made the information difficult to access and assess. For clarification, it is necessary to summarise the evidence so that it can receive wider attention and the broad range of support for New Geophysics can be more easily recognised.

## 2. The Range of Evidence for New Geophysics

Zatsepin and Crampin (1997) and Crampin and Zatsepin (1997) suggest that stress-induced deformation of fluid-saturated microcracked rock is caused by migration of pure-fluids along pressure gradients between microcracks at different orientations to the stress-field. Known as Anisotropic Poro-Elasticity (APE), the process is illustrated schematically in Figure 3, which shows horizontal cross-sections of stress-induced modifications to an initially randomly oriented microcracked rock for four values of differential horizontal stress, $S_H$: 0.0, 0.5, 1.0, and 3.0.

Figure 3 shows, top-left, a horizontal cross-section of oriented vertical microcracks at zero horizontal differential stress, $S_H = 0$. At zero differential stress the intergranular microcracks have equal aspect-ratios; since the symmetry of elastic-constants means that hexagons are necessarily isotropic, there is no shear-wave velocity-anisotropy (0%SWVA), and the microcracks are effectively random. Thus the hexagons of microcracks top-left are a small selection of randomly oriented microcracks.

For a small increase of stress, $S_H = 0.5$, top right, some pore-fluids follow pressure gradients between microcracks at different orientations to the stress-field. Crack aspect-ratios are marginally increased parallel to the direction of maximum horizontal stress but

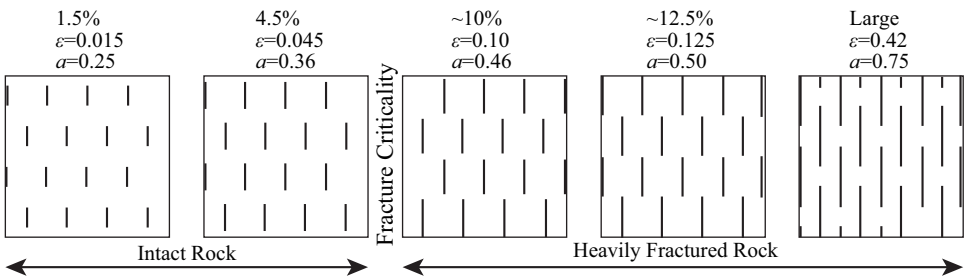


**Figure 2**. Schematic illustration of uniform cross-sections of three-dimensional distributions of penny-shaped microcracks for five percentages of shear-wave velocity-anisotropy (%SWVA). Above each distribution are listed: %SWVA; $\varepsilon$, crack-density; and $a$, crack radius in a unit cube. Fracture-criticality is indicated at ~5%SWVA.

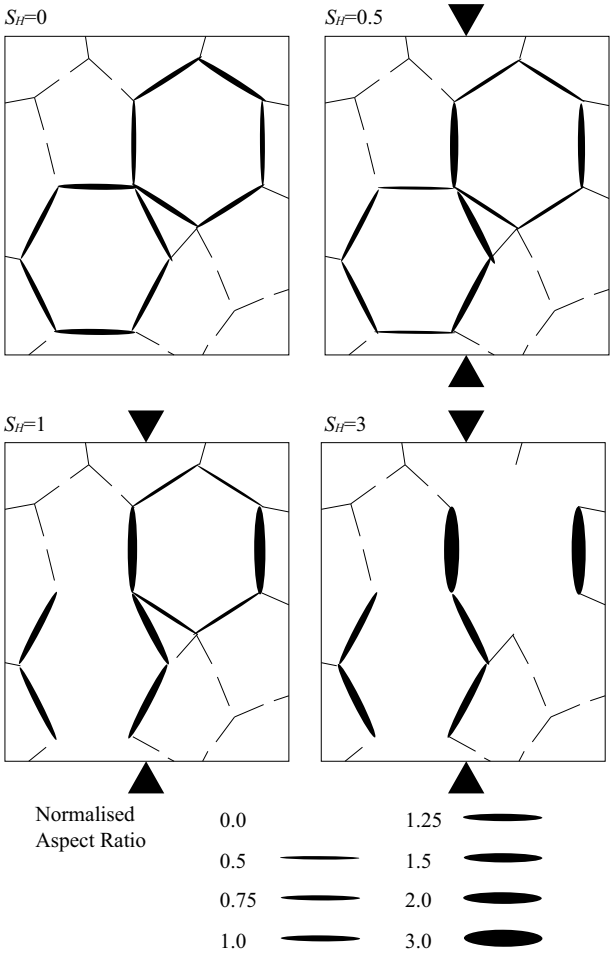


**Figure 3**. Schematic illustration of deformation of microcracked rock by Anisotropic Poro-Elastic (APE). Horizontal cross-section of an initially random distribution of fluid-saturated vertical microcracks deformed by four values of horizontal differential stress, $S_H$ = 0, 0.5, 1.0, 3.0. Behaviour described in text.

as microcracks remain open, the SWS velocity-anisotropy is negligible (~0%SWVA). As stress increases, (bottom left) microcracks first begin to close at a differential stress, normalised to $S_H$ = 1, for crack faces normal to the direction of maximum horizontal stress (Crampin, 1994; Crampin and Peacock, 2008, Crampin and Gao Y, 2013), and anisotropy jumps from zero to approximately the 1.5%SWVA minimum observed in the Earth (Figure 2). As stress increases, $S_H$ = 3 (bottom right), aspect-ratios and SWVA continue to increase until at fracture-criticality (5%SWVA, not illustrated), the percolation threshold is reached (Crampin and Zatsepin, 1997), where the microcracks are approximately aligned parallel to the direction of maximum horizontal stress, and the rock will fracture and an earthquake will occur if there is any disturbance. Note that the distinctive minimum ~1.5%SWVA was recognised in the field (Crampin, 1994) before the behaviour was modelled by APE in Figure 3 (Crampin and Zatsepin, 1997).

APE-modelling (Figure 3) of the deformation of the stress-aligned fluid-saturated microcracks in the New Geophysics of a microcracked rock mass, approximately matches the large number of phenomena listed in Table 1 along thousands-to-millions of individual source-to-receiver ray paths. The match is approximate because the details of the stress-induced behaviour of *in situ* microcracks in the interior of the Earth are not known and only inferred from observations of SWS. The list in Table 1 could easily be extended. The phenomena range from simple observational evidence: such as the minimum ~1.5%SWVA observed in all types of *in situ* rocks from 20%-porosity sedimentary rocks to 2%-porosity igneous and metamorphic rocks (Crampin, 1994; Crampin and Peacock, 2008); to the maximum ~4.5%SWVA similarly widely observed; and the more subtle reasons such as the linearity of the Gutenberg-Richter magnitude log-frequency relationship (Crampin and Gao Y, 2015); and other phenomena some of which are discussed in Sections 3.1 to 3.7, below. None of these can be explained by conventional sub-critical geophysics without the introduction of innumerable special cases.

## 3. Direct Evidence for New Geophysics

We summarise a range of phenomena that provide direct evidence for the utility of the New Geophysics of critical distributions of fluid-saturated stress-aligned microcracks.

### 3.1 Using APE to Model the Waveforms Before and After High-Pressure $CO_2$-Injections

Angerer et al. (2002) used APE to model the waveforms of three-component reflection surveys in a fractured dolomite reservoir before and after both critically-high-pressure and low-pressure $CO_2$-injections in the Reservoir Characterisation Project (RCP) of Colorado School of Mines in Vacuum Field, New Mexico (Roche et al., 1997). APE-modelling accurately predicted the changes in SWS following both injections. Referring to the critically-high-pressure injection: Figure 4 shows, top row, two-way record sections of S1- and S2-oriented shear-wave reflections and P-wave reflections (before injection) from shear-wave vibrators. The reflections were shot in a 25 m-grid of three-component recorders and shear-wave vibrators. S1- and S2-waves are the faster and slower split shear-waves, which are oriented in directions of the maximum and minimum horizontal-stress, respectively (Angerer et al., 2002). The first five traces are the observed traces at the nearest field recorders, and the last three traces are APE-modelled traces for the known velocity structure with a microcrack structure designed to match the existing crack-induced 2%SWVA. The top and bottom of the intended injection zone (identified by RCP) are marked by arrows to the right, with a 172 ms delay for S1 and 174 ms for S2, showing that S1 is the faster split shear-wave. The match of observations to APE-modelled traces is good, where the modelled seismograms have omitted reverberations.

The bottom two sections show the same recorder orientations and APE-modelling following a $CO_2$-injection of 17 MPa over-pressure into the (arrowed) target zone. The five observed traces show differences particularly in the target zone. The APE-modelled traces take the theoretical model for the pre-injection values, in the top record sections, and theoretically introduce the 17 MPa injected pore-pressure into the APE modelling. Again, the match of observations to APE-modelled traces is good, showing the success of the APE-modelling procedure and confirming New Geophysics. This is a demonstration of the applicability of APE-model-

**Table 1.** Evidence supporting APE and the crack-critical New Geophysics (after Crampin and Gao Y, 2013)

| | Evidence inexplicable in terms of conventional sub-critical geophysics* | Ref.† |
|---|---|---|
| 1) | Shear-wave splitting is observed in almost all *in situ* rocks in the crust and upper mantle. | [1, 2, 3] |
| 2) | There is a minimum SWVA of ~1.5% in almost all *in situ* rocks. | [1, 2, 3] |
| 3) | There is a maximum SWVA of ~5.5% in ostensibly unfractured rock. | [1, 2, 3] |
| 4) | Fracture-criticality limit of SWVA is ~5.5% in *in situ* rocks independent of rock-type, geology, tectonics, and porosity, etc, where SWVA of ~5.5% is the percolation threshold for parallel cracks. | [1, 2, 3] |
| 5) | High pore-fluid pressures induce 90°-flips in polarizations of the faster split shear-waves. | [4, 5] |
| 6) | Explains the large ("±80%") scatter in shear-wave time-delays above small earthquakes. | [5, 6] |
| 7) | Effects of $CO_2$-injections on seismic reflection surveys modelled by APE. | [4, 5, 6] |
| 8) | Stress-accumulation observed before earthquakes. | [7, 8, 9] |
| 9) | Time, magnitude, and impending fault-break successfully stress-forecast in real time. | [8, 9] |
| 10) | Stress-relaxation (crack-coalescence) observed before earthquakes. | [2, 10] |
| 11) | Stress-accumulation observed before volcanic eruptions. | [2, 7, 8] |
| 12) | Extreme sensitivity: stress-variations observed in Iceland two and a half years before the Sumatra Earthquake at the width of the Eurasian Plate (~10,500 km) from Indonesia. | [11] |
| 13) | Explains how a stressed rock differs from an unstressed rock. | [12] |
| 14) | Explains how the enormous stress-energy before a large earthquake accumulates without inducing smaller earthquakes. | [12] |
| 15) | Explains why initial stress drop at an earthquake is small (typically 2 to 4 MPa) and independent of earthquake magnitudes which may vary by over 10 orders of magnitude. | [12] |
| 16) | Explains how irregular fault-planes slip when constrained by enormous lithostatic stress. | [12] |
| 17) | Explains why we cannot deterministically predict but can stress-forecast the time, magnitude, and fault-break of impending earthquakes. | [12] |
| 18) | Explains why the Gutenberg and Richter (1956) relationship between logarithms of cumulative frequencies of earthquakes and earthquake magnitudes is linear. | [13] |
| 19) | Partly explains why, despite huge investment, average recovery is less than 40% of in-place oil. | [14] |

* Without innumerable special cases.
† References: [1] Crampin(1994, 1999); [2] Crampin and Peacock (2008); [3] Crampin and Zatsepin (1997); [4] Angerer et al. (2002); [5] Crampin et al. (2002); [6] Crampin et al. (2004a); [7] Volti and Crampin (2003); [8] Crampin et al. (1999); [9] Crampin et al. (2008); [10] Gao Y and Crampin (2004); [11] Crampin and Gao Y (2012); [12] Crampin et al. (2013); [13] Crampin and Gao Y (2015); [14] Crampin (2006).

ling to the New Geophysics. Note that the velocities of P–waves are insensitive to fluid-saturated microcracks (Crampin and Kirkwood, 1981) and the time-lapse P-wave reflections show negligible differences.

An additional distinctive feature is also observed and modelled. Following the high-pressure $CO_2$-injection, the time-delays between the top and bottom of the injection zone are now 204 ms for S1 and 184 ms for S2, showing that after the high-pressure injection the S2-wave has become the faster SWS phase. There has been what Angerer et al. (2002) call a '90°-flip' in shear-wave polarisations. Such flips have also been observed in a walk-away vertical-seismic-profile in a high-pressure Caucasus reservoir (Crampin et al., 1996), and immediately above swarms of small earthquakes when the shear-waves pass though the high-fluid-pressure envelopes surrounding all seismically-active faults (Crampin et al., 2002, 2003, 2004a). Thus APE identifies and models an unexpected feature of the effects of critically high-pressure pore-fluids in hydrocarbon reservoirs, and earthquake fault monitoring, which provide strong support for the validity of New Geophysics. These phenomena match properties P2 Monitorability, P3 Uniformity, P4 Calculability, and P5 Predictability in Table S1.

### 3.2 Extreme Sensitivity where the SWS Shows the Effects of Seismicity Equivalent to a *M* 3.5 Earthquake at ~70 km from the Source Zone

Figure 5 shows observations from the SMSITES experiment (Crampin et al., 2003). A shear-wave source in a cross-hole seismic experiment excited SV- and SH-waves at 500 m-depth between two boreholes 315 m-apart, adjacent (at ~100 m-distant) and parallel to the Húsavík-Flatey Transform Fault (HFTF) of the Mid-Atlantic Ridge (MAR) as it runs onshore in Northern Iceland. The downhole-orbital-vibrator source (DOV) (Walter et al., 2003) was pulsed in sweeps to 250 Hz over 12–20 s, two or three times each minute, and stacked every 100 sweeps for 24 hours each day.

Figure 5 shows observations over 13 days, 11–24 August 2001 (with two short breaks for equipment assessment). The figure shows: (a) P-wave travel times, with an immediate 5 ms increase in travel time, followed by a linear decrease in travel time over nine days with 6% velocity anisotropy; (b) a 2 ms (2%SWVA) SWS difference in SV- and SH-wave travel times showing a classic 'S'-shaped stress-relaxation decrease in travel times over five days; (c) 10% shear-wave velocity-anisotropy in SV-SH travel-times; (d) NS and

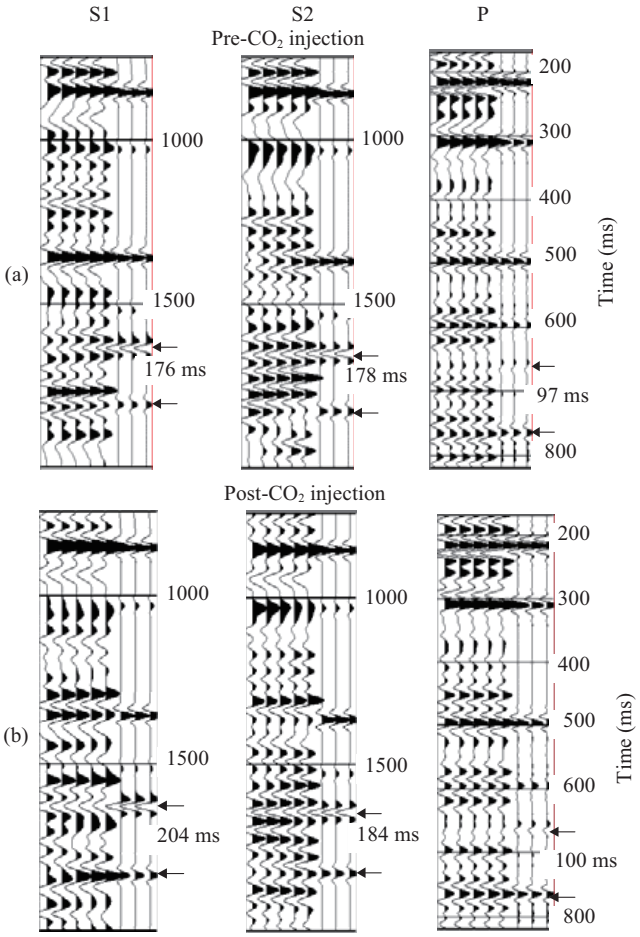


**Figure 4**. (a) Pre-injection waveforms of a multi-component nearly-vertical ray reflection survey near the centre of Vacuum Field, New Mexico, carbonate reservoir (Angerer et al., 2002). S1-, S2-, and P-waves are reflection sections with mutually orthogonal polarisations, where the horizontals S1, and S2, have been rotated into the split shear-wave polarisations parallel and perpendicular to the direction of maximum horizontal stress, respectively. Left-hand (LH) five traces are observed waveforms at adjacent recorders 17 m apart, and the right-hand (RH) three traces are synthetic seismograms modelled by APE to match the shear-wave and SWS arrivals. Top and bottom of injection zone for shear waves are marked by arrows with time-delays in ms/km. (b) Post-injection waveforms two-weeks after a high-pressure $CO_2$-injection. Again, the LH traces are observations and RH traces are synthetic seismograms modelled by APE with the structure from (a) and an injection pressure of 6.4 MPa (after Angerer et al., 2002).

EW Global Positioning System (GPS) measurements showing an immediate abrupt NS pulse with following displacements compatible with a right-lateral 4 mm movement of the approximately EW HFTF; (e) water pressure showing bi-diurnal tidal oscillations at 33 m-depth in a water-well on the island of Flatey immediately above the HFTF, showing an impulsive 1 m drop in water-pressure lasting five days; and (f) a histogram of small earthquakes within 100 km of SMSITES, Húsavík, Iceland (Crampin et al., 2003).

The histogram (f) records a swarm of 106 small earthquakes ($M$ < 2.5), with an equivalent energy less than a single $M$3.5 earthquake, near the Island of Grímsey, ~70 km NNE of Húsavík, on the Grímsey Lineament of MAR, parallel to HFTF. The onset of the histogram coincides with the beginning of the variations in Figures 5a–5e. The energy-equivalent $M$ 3.5 earthquake is small with a conventional source zone of a few hundred metres in radius. Thus the observations in Figure 5, at ~70 km from the earthquake source, are at hundreds of times the radius of the conventional earthquake source zone, and show the extreme sensitivity expected in New Geophysics (property P8 Sensitivity, Table S1). These various phenomena match properties P2 Monitorability, P3 Uniformity, P4 Calculability, P5 Predictability, P7 Universality, and P8 Sensitivity in Table S1.

Note that, as both principal stresses and recording directions at SMSITES are aligned approximately NS and EW, the recording geometry is in nearly singular directions. Consequently, numerical modelling of the phenomena would be ambiguous and impossible to resolve.

### 3.3 Real-Time Stress-Forecast, where the Time, Magnitude, and Fault Break of An *M* 5 Earthquake was Successfully Stress-Forecast Three Days Before it Occurred

Figure 6 shows SWS time-delays measured at Station BJA of the South Iceland Lowland seismic network of the Iceland Meteorological Office (IMO) by visual inspection of polarisation diagrams for the four years, 1996–1999. BJA is sited in the SW Iceland transform zone of MAR which generates nearly continuous swarms of small earthquakes in the shear-wave window of BJA suitable as sources for monitoring SWS (Volti and Crampin, 2003). (Iceland is in a unique location as the only place known to the authors where the seismicity of mid-oceanic-ridge transform-zones runs onshore providing suitably-persistent swarms of small earthquakes for *routine* monitoring of SWS.) The lower half of Figure 6 shows measured time-delays in Band-1 directions in the shear-wave window, where Band-1 directions are sensitive to crack aspect-ratios that change with varying stress (Crampin, 1999). Note that the "±80%" scatter in Figure 6 (Table 1, Item 6) in the SWS time-delays is due to 90°-flips in shear-wave time-delays caused by shear-waves from the SWS source passing through the critically high-fluid-pressure envelopes surrounding all seismically-active faults (Crampin et al., 2002, 2004a, also see Sections 3.1 and 3.2, above).

The Band-1 SWS time-delays show stress-accumulation before the October, 1996 Gjàlp fissure eruption beneath the Vatnajökull Ice Cap (Volti and Crampin, 2003), followed by a ~2 ms/km/year decrease over two years, interpreted as the response of the MAR to the stress released by the Gjàlp eruption. Stress-accumulations before five smaller earthquakes are superimposed on the two-year decrease (Figure 2, No. 1b in Crampin et al., 2015, henceforth referred to as Paper 1). In 2008 it was recognised that stress was accumulating preparatory to an impending earthquake, and on 10th November, 1998, Edinburgh University (EU) sent an email stress-forecast to IMO: "… *an event could occur any time between now ($M \geq 5$) and the end of February ($M \geq 6$).*" Three days later on 13th November, 1998, IMO emailed EU: "… *there was a magnitude 5 earthquake just near to BJA … this morning 10.38 GMT.*" (Crampin et al., 1999, 2004b, 2008). Co-author Ragnar Stefánsson had previ-

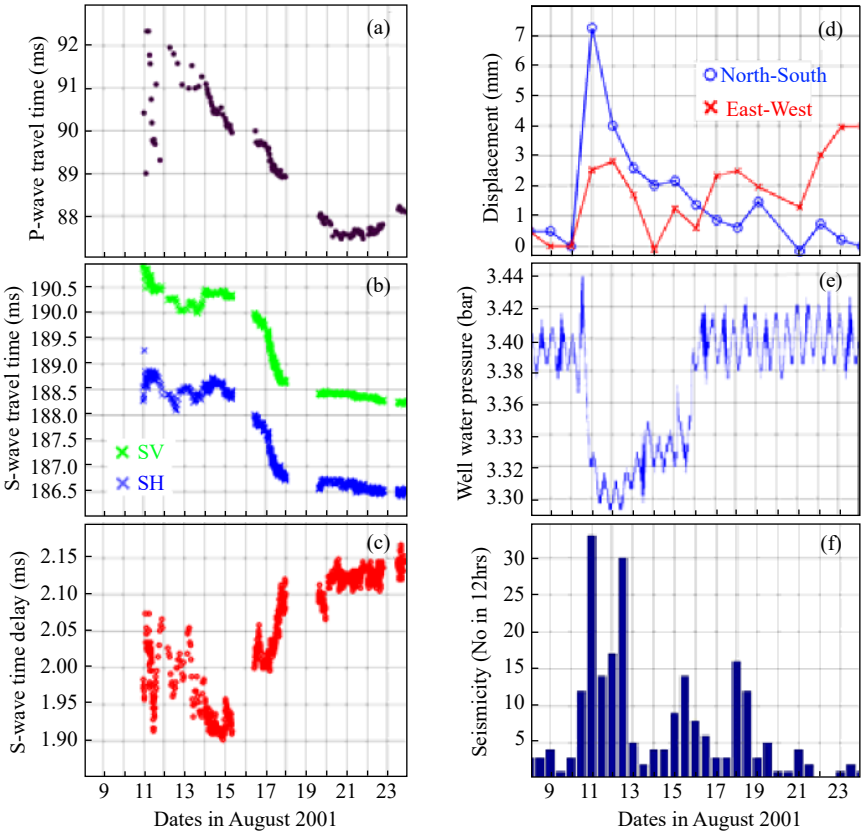


**Figure 5**. Observations at a prototype Stress-Monitoring Site (SMS) (Crampin et al., 2003). (a), (b), and (c) are travel times in ms of P-, SV-, and SH-waves, and SV-SH anisotropy, respectively, at 500 m-depth between boreholes 315 m-apart. The directions are parallel to and about 100 m south of the Húsavík-Flatey Transform Fault (HFTF). Shear-waves are polarised SV- and SH-waves propagating horizontally in a symmetry direction of the stress-field. Also shown are (d) NS and EW GPS displacements in mm; and (e) water pressure measured in bars at 33 m-depth in a water-well immediately above the HFTF, where the bi-diurnal oscillations are ocean tides, and the abrupt decrease 'pulse' is equivalent to a 1 m fall in water level. The onset of variations in (a) to (e) correlate with (f) a histogram of small earthquakes within 100 km of SMS, where the initial concentration is 106 small earthquakes ($M$ <2.5) on a parallel transform fault ~70 km NNW of SMS, whose total energy is approximately equivalent to one $M$ 3.5 event.

ously correctly forecast the fault-break, following an earlier preliminary stress-forecast. Stefánsson correctly suggested that the impending earthquake would be likely to occur on a neighbouring fault where low-level seismic activity was still continuing following an $M$ 5.1 earthquake six months earlier.

We suggest that this 1998 $M$ 5 earthquake in SW Iceland is the first scientifically stress-forecast earthquake (Crampin et al., 1999, 2004b, 2008). It is different to several less-accurate probabilistic estimates by other geoscientists such as Kossobokov (2013). Note that we use the term *stress-forecasting* of earthquakes, rather than predicting or forecasting earthquakes, to empathise the different methodology.

Figure 7a (from Gao and Crampin, 2004) expands the variations of SWS time-delays in Figure 6 before the stress-forecast earthquake in a convenient format for displaying stress-forecasts as used in Figure 1 in Paper 1 and in Gao and Crampin (2004). Gao Y and Crampin (2004) were the first to recognise stress-relaxation (crack-coalescence) decreases in SWS time-delays. Consequently the successful stress-forecast (Crampin et al., 1999, 2004b, 2008) was based only on the stress-accumulation increases in the left-hand-side diagram of Figure 7a. The SWS and stress-forecast earthquake was introduced clearly in Gao Y and Crampin (2008). Since earthquake prediction in conventional sub-critical geophysics impossible (Geller, 1997; Geller et al., 1997), this stress-forecast, and the retrospective stress-forecasts in Paper 1 and in Sections 3.4 and 3.5, below, are strong evidence for the critical New Geophysics. These phenomena match properties P2, P3, P4, P5, P7, and P8 in Table S1.

Note that Figure 7a is copied from Gao Y and Crampin (2004) who used a different lower-magnitude-limit data set for IMO earthquakes than that used by Volti and Crampin (2003) in Figure 6. Consequently, although the SWS effects in Figure 7a are compatible with Figure 6, the exact time-delay data in the figures are marginally different. Figures 7a and 7b are discussed in Section 3.6, below.

### 3.4 Similar Characteristic Behaviour to that Seen in the One Successful Stress-Forecast (Figure 7a) Seen Retrospectively Before ~16 Other Earthquakes

Paper 1 presents all known retrospective stress-forecasts and the one real-time stress-forecast in a normalised format that allows the overall effects to be compared. Characteristic stress-accumula-

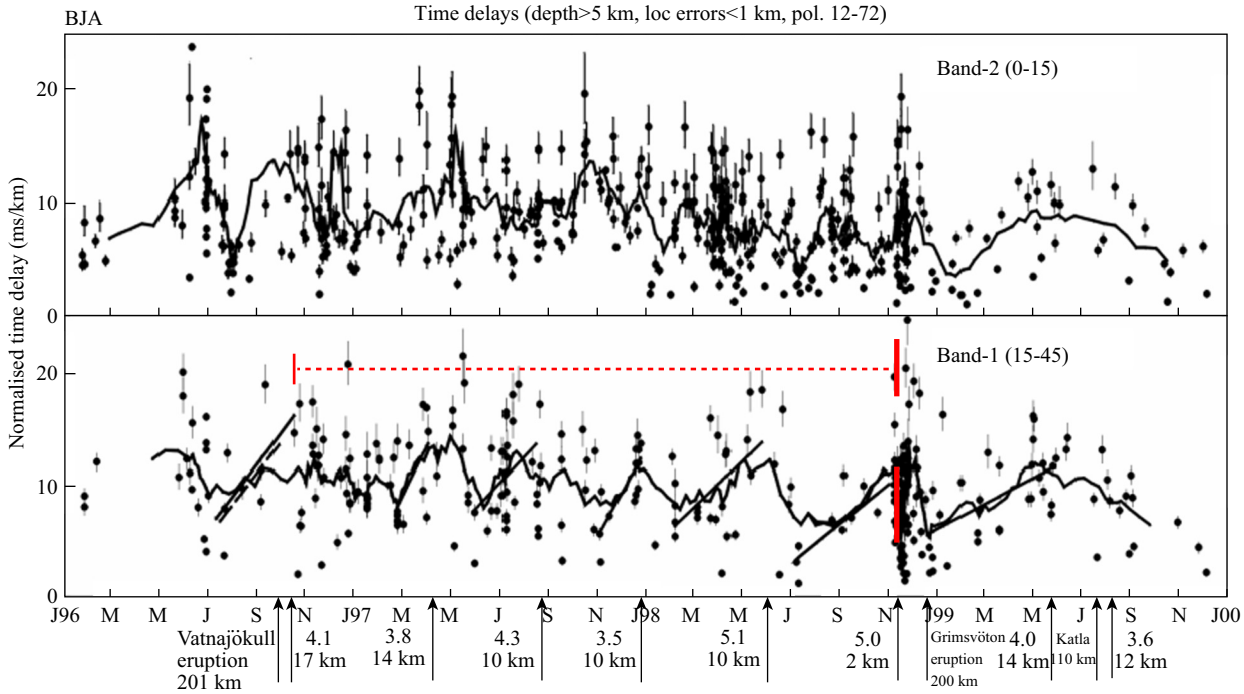


**Figure 6**. Variations of SWS time-delays over four years (1996–1999) at IMO seismic station BJA in SW Iceland (after Volti and Crampin, 2003). Lower diagram is arrivals in Band-1 directions (sensitive to stress changes), and upper diagram is arrivals in Band-2 directions (sensitive to changes in both stress and crack density) (Crampin, 1999). Both diagrams have nine-point moving averages through the data points. Straight lines are least-squares averages of time-delays before larger earthquakes marked below. The dashed line marks time interval of two-year decrease of time-delays of ~2 ms/km/year following the October, 1996, Gjàlp volcanic eruption beneath the Vatnajökull Ice Cap.

tion variations of SWS time-delays similar to the successful stress-forecast in the right-hand-side of Figure 7a are observed retrospectively before 16 other earthquakes (Figure 1, Paper 1) and three volcanic eruptions (Figure 2, Paper 1). The 16 earthquakes where stress-accumulation has been observed retrospectively (Table 2), range from an $M$ 1.7 swarm event in Northern Iceland (Gao Y and Crampin, 2004) to the 2004, $M_w$ 9.2, Sumatra Earthquake (Crampin and Gao Y, 2012). Observations of stress-accumulation are considered to be robust and have always been observed whenever appropriate source-to-receiver geometry and large or larger earthquakes are available (Gao Y and Crampin, 2008). There are no known exceptions where stress-accumulation has not been observed when suitable source-to-recorder conditions exist (Crampin and Peacock, 2008).

Observations of stress-relaxation (and implied crack-coalescence) are less robust. Of the 16 earthquakes where stress-relaxation has been identified in Table 2 (plus the one successful stress-forecast), only 11 (65%) show stress-relaxation decreases that could be used for confirming stress-forecasts if SWS time-delays had been monitored in time. Observations of stress-relaxation in real-time require sufficient small events in the shear-wave source swarm immediately below the monitoring station before the time of the impending earthquake, and these are not always available. Additionally, stress-relaxation decreases may be disturbed by anomalous high-pore-fluid-pressures known to be present on all seismically-active faults, causing 90°-flips in shear-wave polarisations and ±80% scatter in SWS time-delays (Crampin et al., 2002, 2004a) so that stress-relaxation may be hidden or uninterpretable. These phenomena match properties P2 Monitorability, P3 Uniformity, and P7 Universality of Table S1.

### 3.5 Extreme Sensitivity where Stress-Accumulation and Stress-Relaxation were Observed in Iceland Before the 2004 $M_W$ 9.2 Sumatra Earthquake at a Distance of ~10,500 km, the Width of the Eurasian Plate, from Indonesia

From September 2002, Crampin and Gao Y (2012) reported very gradual stress-accumulation increases at seven stations of the IMO seismic network in Iceland (Figure 1, Nos. 18a-to-18g, Paper 1). The extreme sensitivity to stress changes had not been recognised at that time and the gradual increase suggested stress-accumulation before a large ($M$ ~7, say) earthquake in Iceland. Ten stress-forecasts (Table 3) were emailed to IMO from 13th September 2002, updated every few months, stress-forecasting an impending $M$ ~7 earthquake in Iceland. (Seismic stations in Table 3 are listed in bold font for southern stations, and regular font for northern stations, in an attempt to locate evidence of proximity of the cause of the increase–no proximity was indicated.) In September, 2004, marginally decreasing time-delays suggested that the time of the impending earthquake was approaching. However, it was only after the $M_W$ 9.2 Sumatra Earthquake on 26th December 2004 had occurred that the extreme sensitivity was recognised and the gradual stress-accumulation in Iceland attributed to stress-accumulation before the $M_W$ 9.2 Sumatra Earthquake in Indonesia at a distance of ~10,500 km (approximately the width of the Eurasian Plate) from Iceland (Crampin and Gao Y, 2012). These

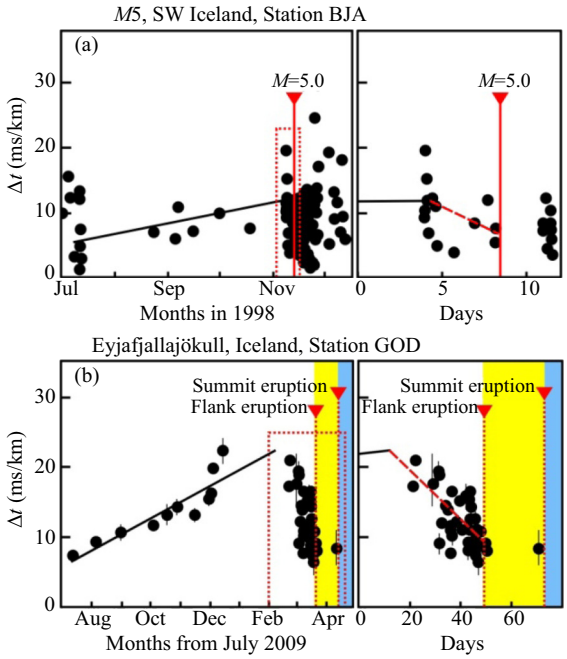


**Figure 7**. Comparison of variations in SWS time-delays before (a) earthquake and (b) volcanic eruption in SW Iceland. (a) Detailed plot July, 1998 to December, 1998 of variations of SWS time-delays in Band-1 at Station BJA in Figure 6 before the stress-forecast *M* 5 earthquake of 13th November, 1998 in SW Iceland (Crampin et al., 1999), where the left-hand side shows least-squares line through the stress-accumulation increase before the earthquake lasting about four months. The right-hand side is an expansion of the red dotted box in the left-hand side showing the stress-relaxation decrease starting about four days before the earthquake (after Gao Y and Crampin, 2004). (b) Plot of variations of SWS time-delays at Station GOD showing stress-accumulation and stress-relaxation before the 2010 Eyjafjallajökull eruption Iceland in the same format as (a). The flank eruption in yellow lasted ~20 days, and the summit eruption in blue lasted 39 days (after Liu S et al., 2014).

phenomena match properties P2 Monitorability, P3 Uniformity, P7 Universality, and P8 Sensitivity of Table S1. Such extreme sensitivity (P8) is not expected in conventional sub-critical geophysics and is a direct confirmation of the critically-microcracked New Geophysics.

### 3.6 Nearly Identical SWS Behaviour Before Earthquakes and Volcanic Eruptions

Figure 7b shows variations in SWS time-delays at seismic Station GOD before the 2010 Eyjafjallajökull volcanic eruption in Iceland (Liu S et al., 2014). The eruption was unusual in having two episodes of comparatively long duration (Gudmundsson et al., 2011): a flank eruption of ~20 days from April 14, 2010 (coloured yellow in Figure 7b) and a summit eruption of 39 days (coloured blue).

The SWS variations at GOD in Figure 7b are compared with the SWS variations in Figure 7a for the successfully stress-forecast earthquake *M* 5 November 13, 1998 at Station BJA (Table 1, No. 10a, Paper 1), which is some 90 km west of GOD. The variations of SWS time-delays before the earthquake (a) and before the eruption (b) show strong similarities. They both show an approximately linear (stress-accumulation) increase followed by an approximately linear (stress-relaxation) decrease after an abrupt change of slope. Both earthquake and eruption occur when the level of SWS time-delays is approximately at the level at the start of the stress-accumulation increase. This means that the eruption could have been stress-forecast to within one or two days (Section 5.2 of Paper 1–Liu S et al., 2014).

As we have shown (Figure 3a, Paper 1), the slopes of the logarithms of the durations of the stress-accumulation increases before earthquakes are approximately proportional to the magnitudes of the earthquakes. Since the 'size' of volcanic eruptions depends on many chemical, petrological, and tectonic factors, there is no unique scale for the size of volcanic eruptions corresponding to the magnitude of earthquakes (Francesca Bianco, personal note). Figure 7a shows that the logarithm of the duration of stress-accumulation is proportional to the earthquake magnitude. The similarity of the duration of stress-accumulation before earthquakes (17 earthquakes in Figure 1, Paper 1) to the duration before volcanic eruptions (three eruptions in Figure 2, Paper 1) suggests that logarithms of the duration of stress-accumulation before eruptions is a potential means of classification for scaling the size of volcanic eruptions in some circumstances. By implication, this would correlatethe energy of an eruption with the proceeding stress-accumulation.

These phenomena match properties P1 Self-similarity, P2 Monitorability, P3 Uniformity, P4 Calculability, P5 Predictability, and P7 Universality of Table S1.

### 3.7 Fundamental Questions (Conundrums) about Earthquakes Resolved by New Geophysics

Crampin et al. (2013) suggested four fundamental questions (conundrums) about earthquake behaviour that are inexplicable in terms of conventional sub-critical geophysics, but are resolved by the properties of the critical New Geophysics. We summarise the resolution of the four conundrums and present a fifth conundrum:

#### 3.7.1 Conundrum C1: How does stressed rock differ from unstressed rock?

Observations of SWS show that almost all *in situ* rock contains anisotropic distributions of stress-aligned microcracks where pore-fluid pressures, in microcracks with varying aspect-ratios, balance the external stress-field, as in Figure 3 (Crampin and Zatsepin, 1997). These aligned microcracks alter the effective anisotropic elastic constants by largely elastic processes (fluid-movement by flow or dispersion along pressure gradients) which can be monitored by SWS. Note that SWS does not measure *in situ* stress: changes in SWS time-delays and polarisations monitor the effects of changes of stress on microcrack geometry.

#### 3.7.2 Conundrum C2: How do *in situ* rocks accumulate the enormous stress-energy released by large earthquakes?

Observations of SWS show that the range of stress-accumulation before fracture-criticality has SWVA values from ~1.5% to ~4.5% (Crampin, 1994; Crampin and Peacock, 2008). We see from Figure 3

**Table 2.** Earthquakes which have been retrospectively stress-forecast from stress-accumulation where stress-relaxation with crack-coalescence has or has not been identified (after Paper 1)

| | Magn.[$] | Year | Earthquake identifier | Recording location | Stress-rel. | Ref. [†] |
|---|---|---|---|---|---|---|
| 1 | $M_I$ 1.7 | 2002 | Swarm event, N Iceland | N Iceland | yes | [1] |
| 2 | $M_I$ 2.5 | 2002 | Swarm event, N Iceland | N Iceland | yes | [1] |
| 3 | $M_I$ 3.4 | 1997 | SW Iceland | SW Iceland | – | [2] |
| 4 | $M$ 3.6 | 1992 | Dongfang, Hainan | Hainan, China | – | [3] |
| 5 | $M_d$ 3.8 | 1982 | Enola Swarm | Arkansas, USA | yes | [4] |
| 6 | $M_I$ 3.8 | 1997 | SW Iceland | SW Iceland | – | [2] |
| 7 | $M_L$ 4.0 | 1988 | Parkfield, California | California, USA | – | [5] |
| 8 | $M_I$ 4.4 | 1997 | SW Iceland | SW Iceland | yes | [2] |
| 9 | $M_I$ 4.9 | 2002 | Grímsey Lineament | N Iceland | yes | [6] |
| 10 | $M_I$ 5.1 | 1998 | SW Iceland | SW Iceland | – | [2] |
| 11 | $M$ 5.9 | 1992 | Shidan, Yunnan | Yunnan, China | yes | [7] |
| 12 | $M_S$ 5.9 | 1999 | Xiuyan, Liaoning | Liaoning, China | – | [8] |
| 13[‡] | $M_S$ 6.0 | 1986 | North Palm Springs | California, USA | yes | [9] |
| 14 | $M_S$ 6.6 | 2000 | SW Iceland | SW Iceland | yes | [10] |
| 15 | $M_W$ 7.7 | 1999 | Chi-Chi | Taiwan | yes | [11] |
| 16 | $M_W$ 9.2 | 2004 | Sumatra | Iceland | yes | [12] |

[$] Magnitudes are listed as originally reported: many are IMO body-wave magnitude $M_I$.
[‡] Earthquake where changes in SWS were first recognised (Peacock et al., 1988).
– Absent or unreliable stress-relaxation.
[†] References: [1] Gao Y and Crampin (2004); [2] Volti and Crampin (2003); [3] Gao Y et al. (1998); [4] Booth et al. (1990); [5] Liu Y et al. (1997); [6] Gao Y and Crampin (2006); [7] Gao Y and Crampin (2003); [8] Tai LX et al. (2008); [9] Peacock et al. (1988); Crampin et al. (1990); Crampin et al. (1991); [10] Wu J et al. (2006); [11] Crampin and Gao Y (2005); [12] Crampin and Gao Y (2012).

that a small change in crack aspect-ratios (a small change of stress) takes rock from being unfractured to having microcracks so closely-spaced they verge on failure at fracture-criticality in critical-systems (Davies, 1989b). This means that the huge stress-energy accumulated before a large earthquake is necessarily spread very thinly over very substantial volumes of rock (Crampin and Gao Y, 2012). It is only when the stress-field senses a weakness and microcracks begin to coalesce around the impending fault-plane that the particular fault-plane is identified and an earthquake releases stress-energy accumulated in the surrounding rock mass for the appropriate earthquake magnitude.

#### 3.7.3 Conundrum C3: Why is the stress drop at earthquakes small and independent of earthquake magnitude?

Comprehensive surveys show that observed stress drops at earthquakes are typically small and independent of the magnitude of the impending event (Allmann and Shearer, 2009; Baltay et al., 2011). The stress-accumulation and stress-relaxation in Figures 7a and 7b (and throughout the many images in Figures 1 and 2, Paper 1) show that impending earthquakes and volcanic eruptions occur (after the stress-relaxation decrease), when the inferred value of stress is close to the value at the beginning of the initial stress-accumulation increase. This suggests, and the observations of Savage and Brodsky (2011) confirm, that there are similar fracture densities (#/m$^3$) with similar physical processes, and consequently similar stress drops, before both large and small earthquakes.

#### 3.7.4 Conundrum C4: How do rough and irregular fault planes slip when constrained by enormous lithostatic pressures?

APE-modelling demonstrates that the ±80% scatter of SWS time-delays above small earthquakes is caused by 90°-flips in SWS polarisations as shear waves pass through the critically-high pressure fluid-envelopes surrounding all seismically active faults (Crampin et al., 2002, 2004a). Since the average microcrack diameter in Figure 3 is probably less than 2 mm, the inferred crack densities of 0.015 to 0.045 mean that in *in situ* rock there may well be more than 100 deformable microcracks per cubic centimetre. Each microcrack may make only limited adjustments, but when microcracks are so numerous and every microcrack responds to local changes of stress by modifying its aspect-ratio (Crampin and Zatsepin, 1997), the total adjustment may be substantial. This makes *in situ* microcracked rock extremely compliant, and allows rock around fault-breaks to readily adjust to rugosities and changes of curvature, particularly in the critically-high pressure fluid-envelopes expected around seismically active fault-planes (Crampin et al., 2002, 2004a).

We also present a further conundrum not discussed by Crampin et al. (2013):

**Table 3.** Summary of emailed stress-forecasts (SF) from University of Edinburgh (EU) to Iceland Meteorological Office (IMO) (after Crampin and Gao Y, 2012)

| | Date | Seismic stations with stress-accumulation | Seismic stations with stress-relaxation | a) Smaller-Earlier to Larger-Later window.<br>b) Estimate of location.<br>c) Plots of duration/magnitude. |
|---|---|---|---|---|
| SF1 | 13/09.2002 | **BJA, SAU***,<br>BRE | None reported | a) *M*5.6 soon or *M*6+ in 6 months.<br>b) no estimate.<br>c) no plots. |
| SF2 | 11/11.2002 | **BJA, SAU**,<br>BRE, FLA | None reported | a) *M* 6.6 soon or *M* 7+ in 4 months.<br>b) Húsavík-Flatey Fault or Grímsey Lineament.<br>c) no plots. |
| SF3 | 05/12.2002 | **BJA, SAU**,<br>BRE, FLA | None reported | a) *M* ~ 6.<br>b) Húsavík-Flatey Fault.<br>c) no plots. |
| SF4 | 07/03.2003 | **BJA, SAU, KRI**,<br>BRE, FLA, GRI | BRE, FLA | a) *M* 7 soon or *M* 8 in 5-8 months.<br>b) No estimate of location.<br>c) No plots. |
| SF5 | 04/04.2003 | **BJA, SAU**,<br>BRE, FLA | BRE, FLA | a) *M* 7 soon or *M* 8 within 4-7 months.<br>b) Northern Iceland.<br>c) No plots. |
| SF6 | 18/11.2003 | **BJA, SAU**,<br>BRE, FLA | Not reported | a) *M* 7+ soon or within a few months.<br>b) No estimate of location.<br>c) No plots. |
| SF7 | 05/12.2003 | **BJA, SAU, KRI**,<br>BRE, FLA, GRI, HED | Not reported | a) *M* 7+ soon or within a few months.<br>b) No estimate of location.<br>c) No plots. |
| SF8 | 25/06.2004 | **BJA, SAU, KRI**,<br>BRE, FLA, GRI, HED | Not reported | a) *M* 7+ soon or within a few months.<br>b) No estimate of location.<br>c) Plots of duration/magnitude. |
| SF9 | 29/09.2004 | **BJA, SAU, KRI**,<br>BRE, FLA, GRI, HED | **BJA, SAU, KRI**,<br>BRE, FLA, GRI, HED | a) *M* 7+ imminent.<br>b) Húsavík-Flatey Fault or Grímsey Lineament.<br>c) Plots of duration/magnitude. |
| SF10 | 22/12.2004 | **BJA, SAU, KRI**,<br>BRE, FLA, GRI, HED | **BJA, SAU, KRI**,<br>BRE, FLA, GRI, HED | a) *M* ~ 7 imminent - consistent stress-accumulation and crack-coalescence.<br>b) Somewhere in Iceland.<br>c) Plots of duration/magnitude. |
| ► | **26/12.2004 Sumatra Earthquake** | | | ◄ |

***Bold-face font**: seismic stations in the South Iceland Seismic Zone in SW Iceland. Regular-face font: seismic stations over 300 km to the north, near the Húsavík-Flatey Fault and the Grímsey Lineament.

#### 3.7.5 Conundrum C5: How has conventional purely-elastic geophysics satisfied innumerable investigations of seismic-wave propagation and earthquakes despite the linearity of the Gutenberg-Richter relationship demonstrating that, at some level, the behaviour of seismic waves and earthquakes is incompatible with purely-elastic geophysics?

Crampin and Gao Y (2015) show that the linearity of the Gutenberg-Richter relationship is a result of the criticality of the pervasive distributions of stress-aligned fluid-saturated microcracks. The New Geophysics shows that the Gutenberg-Richter relationship is a result of the manipulations of the fluid-saturated stress-aligned microcracks pervasive throughout the Earth's crust and uppermost ~400 km of the mantle.

As demonstrated by APE, each of these conundrums can be resolved by the manipulation of pore-fluid pressures in the New Geophysics of a critically microcracked crust (Crampin and Gao Y, 2013; Crampin et al., 2013). These various conundrums match the wide range of properties of New Geophysics in Table S1.

## 4. Confirmation of New Geophysics

As with many innovative phenomena, New Geophysics has not been readily accepted. Schopenhauer (1788–1860) wrote "All truth passes through three-stages: ridicule; violent opposition; self-evident." When we were promoting seismic anisotropy and crack-induced SWS thirty to forty years ago it took well-over ten years to pass from ridicule to self-evident (Crampin, 1970; Crampin and King, 1977; Alford, 1986). New Geophysics, which is much more innovative than SWS and less easy to prove, may take longer to gain acceptance. One can only accumulate evidence that is satisfied by New Geophysics that cannot be matched by conventional sub-critical geophysics (except by innumerable special cases). Table 1 lists 19 separate items of evidence (along thousands to

millions of individual source-to-receiver ray paths) supporting the New Geophysics of a critically-microcracked crust and transformative (easy-deformed) upper mantle; these 19 examples could easily be extended.

However, the most definitive diagnostic new-property is the ability to predict (stress-forecast) earthquakes, which is claimed to be impossible in conventional sub-critical geophysics (Geller, 1997; Geller et al., 1997). Thus the evidence in Table 2 (and Figure 1, Paper 1) that variations of SWS time-delays above swarms of small earthquakes monitor stress-accumulation before large or larger earthquakes–so that the time, magnitude, and in some circumstances location, of earthquakes can be stress-forecast–is strong confirmation of the power of a New Geophysics of a critically microcracked crust.

Figures 1 and 2 of Paper 1 show that the behaviour of SWS is similar before both earthquakes and volcanic eruptions (Crampin and Gao Y, 2013). This is confirmed by the strong similarities before the successful stress-forecast earthquake (Figure 7a) (Crampin et al., 1999, 2004b, 2008) and before the Eyjafjajökull flank eruption (Figure 7b) (Liu S et al., 2014). This remarkable similarity is strong confirmation of New Geophysics. Such similarities could occur in conventional sub-critical geophysics only if numerous special cases were devised.

This confirmation of New Geophysics is of similar significance to its unprecedented sensitivity, demonstrated by the SMITES experiment in North Iceland discussed in Section 3.2. In that experiment, the equivalent energy to a small $M$ ~3.5 earthquake energy excites classical stress-relaxation anomalies at a distance of ~70 km, hundreds of times the conventional source radius, a clear confirmation of the sensitivity of the New Geophysics in a critically-microcracked crust.

This extreme New-Geophysics sensitivity (P8, Table S1) is also demonstrated in Table 3 and discussed in Section 3.5, where stress-accumulation and stress-relaxation were recognised by changes in SWS in Iceland before the 2004, $M_W$ ~9.2, Sumatra Earthquake in Indonesia at a distance of ~10,500 km from Iceland (Crampin and Gao Y, 2012).

These are a very large number of different phenomena that cannot easily be explained by conventional sub-critical geophysics, but are directly indicative of the explanatory and predictive power of New Geophysics (Crampin et al., 2013) and its many possible applications, including stress-forecasting of earthquakes, which is thought impossible in conventional geophysics (Geller, 1997; Geller et al., 1997).

## 5. Possible Applications in Hydrocarbon Geophysics

There are also possible applications in hydrocarbon geophysics for which some evidence exists that New Geophysics could be highly useful.

### 5.1 SMORE–(S)lower Production for (M)ore (O)il (RE)covery

One of the characteristics of critical-systems is that the self-similarity and calculability occur only when the complex interactions are responding to slow changes (Bak, 1996; Jensen, 1998). Rapid changes (such as aggressive hydrocarbon production strategies) are likely to produce chaotic deformation that will not be self-similar, easily monitorable, or calculable. This suggests that modelling and calculating the response of hydrocarbon systems will be possible only for slow recovery rates, hence the hypothesis: Slower production for More Oil REcovery (SMORE) (Crampin, 2006).

The question is how slow is slow and how much more is more? The delay between the first and second surveys in Figure 4, which shows the effect of observations and calculations of a high-pressure $CO_2$-injection (Angerer et al., 2002; Crampin and Peacock, 2008), was approximately two weeks and was clearly sufficient time as the results were calculable, but it might have been calculable after days or hours. Note that the slow recovery probably needs to be for the whole production history. Initial aggressive production might so disturb the rock as to render it uncalculable.

There are to our knowledge no estimates of how much more is more. Currently, oil fields frequently recovery less than ~40% of the oil in the reserve. Thus, even a conservative overall increase of 5% (it might be substantially greater) to ~45% of produced oil over possibly marginally longer recovery would be ~12% more oil. This would be additional profit on the initial infrastructure cost of oil rigs and pipe lines at the cost of a slower recovery rate.

### 5.2 SWI–Monitoring Production with Time–Lapse (S)ingle-(W)ell [seismic] (I)maging

The movement of oil/water and gas/water interfaces can be monitored by subtracting record sections before and after some oil field production procedure in *time-lapse seismics*. Success depends on successive records shot with identical source-to-receiver geometry. Such detailed sections are expensive offshore, where many major oil fields are situated, and one of the major expenses is laying areal arrays of permanent sea-floor geophones and hydrophones for optimal time-lapse seismics.

Figure 5 shows time-lapse signals contaminated by substantial temporal variations in seismic travel times over 315 m correlating with ~70 km-distant small-scale seismicity. The effects of stress accumulation before higher seismicity, or volcanic eruptions, are likely to be seen across the whole tectonic plate (Crampin et al., 2003; Crampin and Gao Y, 2012). Note that the effects of the New Geophysics are non-linear, as in the ±80% scatter of shear-wave time-delays observed above all small earthquakes (Crampin et al., 2002, 2004b), and cannot be interpreted by conventional sub-critical techniques. Consequently, any *in situ* measurements necessarily degrade both temporally and spatially as soon they are made, and the longer the ray paths the greater the possible degradation.

One way to limit such degradation is to make and interpret measurements at the time and place (the producing reservoir) they are required by Single-Well Imaging (SWI) (Crampin, 2004, 2006). SWI, illustrated schematically in Figure 8, is where the scattered reflections from a borehole (DOV) source are recorded by three-component recorders behind the casing or tubulars in the same well as the source. There are time-lapse techniques for interpreting the scattered signals in terms of changing background: moving

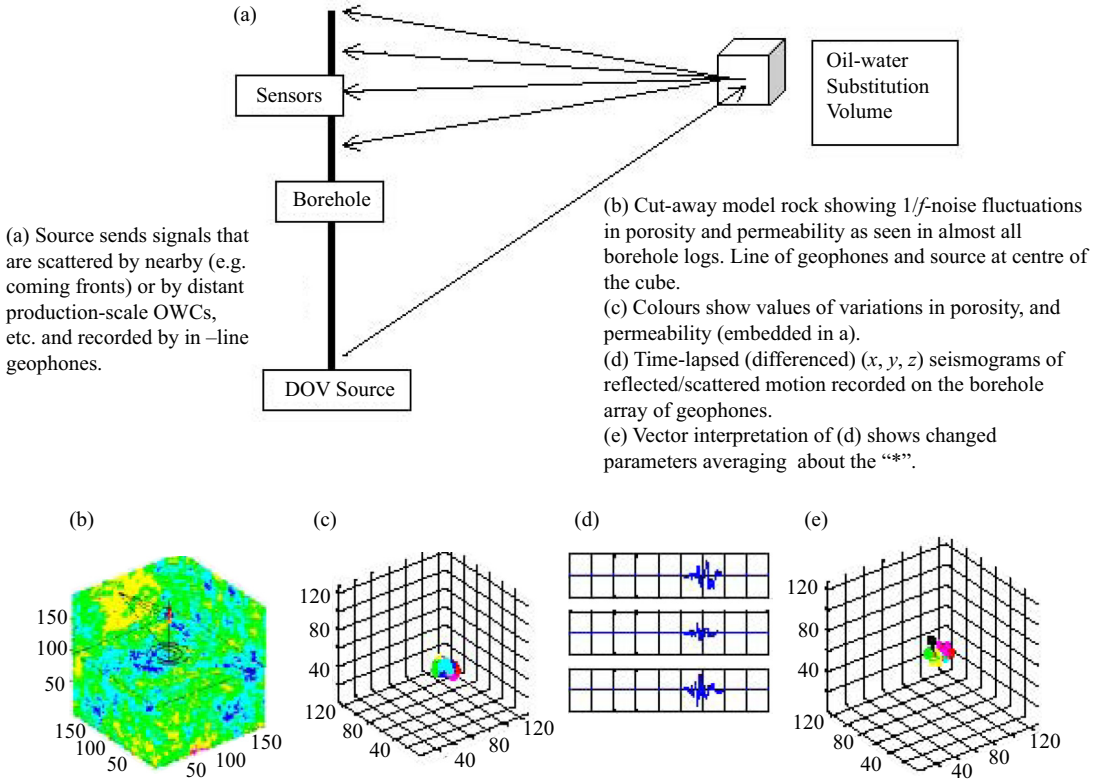


**Figure 8**. Schematic illustration of Single-Well Imaging (SWI). Borehole geophones record signals reflected and refracted from signals generated from pulsed Downhole Oribital Vibrator (DOV) source (Walter et al., 2003) recorded by three-component geophones in the same borehole. (a) Overall geometry of a string of in-hole three-component geophones recording reflections and refractions of a pulsed DOV source in the same borehole. (b) Cut-away model cube of rock showing 1/*f* noise fluctuations in porosity permeability as seen in all borehole logs (Leary, 1991). Vertical string of geophones and DOV source in the centre of the cube. (c) Colours show variations in porosity and permeability embedded in one corner of (a). (d) Time-lapse (differenced) (*x*, *y*, *z*) seismograms of reflected/scattered signals recorded by one of three-component inline geophones. (e) Vector interpretation of (d) showing changes in parameters averaged about '*'. (after Crampin, 2004; Courtesy of Peter Leary).

oil/water contacts for example (Crampin, 2004). SWI limits spatial degradation by recording over the shortest ray path, and limits temporal degradation by recording over the minimum time interval.

One great advantage of SWI is that it is substantially cheaper (~1/100, say) than conventional 4D reflection surveys. Since SWI tracking of fluid fronts is largely independent of geological structure, SWI could eventually replace costly reflection surveys. Note that the results of Figure 8 are derived by processing signals from one three-component geophone. The averaged results from processing a string of geophones would be substantially improved.

Note that Figure 8 shows the principles of SWI. Despite the vector processing being simple and unsophisticated, we suggest that promising results are obtained. Expensive conventional stratigraphic processing and time-lapse surveys are the result of many decades of highly-sophisticated processing and elaborate instrumental installations. We suggest that investment into vector processing would provide substantial improvements to the results of Figure 8.

### 5.3 Optimising Water-Flooding by APE Modelling

The response of the rock mass can be potentially controlled by matching time-lapse shear-wave splitting in 4D reflection surveys or VSPs to APE-modelling (such as in Figure 4) by feedback. This might be important for fluid-injection. If a water-flood operation were initially monitored by appropriate seismic measurements, such as VSPs or potentially SWI surveys, it would be possible to recognise whether cracks had opened in the desired directions to aid fluid-sweep operations. If non-optimal orientations were indicated, different injection procedures could be calculated, modelled, and tested.

This could establish the likelihood of success of a water-flood operation within hours or days of the flood and long before production returns indicated success or failure.

An example on influences of water impoundment to SWS characteristics is reported recently in a reservoir in China (Shao YP et al., 2017). Other possible applications are readily available.

## 6. Conclusions

Table 4 summarises the evidence for New Geophysics in this paper. We have shown that a huge range and variety of phenomena satisfy the APE-modelling criteria in Table 1 and the more detailed analyses reported in Sections 3.1 to 3.7, where the resolution of each example provides more-or-less direct evidence in support of the New Geophysics assumption of a rock mass permeated by critical-systems of microcrack distributions verging on

**Table 4.** Summary of evidence for the New Geophysics reviewed in this paper

| | Evidence | Ref.† |
|---|---|---|
| 1) | A range of 19 different phenomena along thousands-to-millions of individual source-to-receiver shear-wave ray paths that cannot be explained by conventional sub-critical geophysics without innumerable special cases (Table 1). | [1, 2, 3] |
| 2) | Behaviour modelled to match variations of SWS in changing conditions (Figure 4) including 90°-flips in SWS polarisations in critically-high pore-fluid pressures. | [4] |
| 3) | Extreme sensitivity where small magnitude $M\equiv$ 3.5 earthquake energy induced classic stress-relaxation phenomena for seismic velocities between boreholes at ~70 km distance (Figure 5), at least a 100 times source zone-radius in conventional sub-critical geophysics. | [5] |
| 4) | Successful real-time stress-forecast, where the time, magnitude, and fault break of an $M$5 earthquake was successfully stress-forecast three days before it occurred (Figures 6 and 7a). | [6, 7, 8] |
| 5) | Similar characteristic behaviour to Item 4, above, seen retrospectively before ~16 earthquakes where at least 60% could have been successfully stress-forecast had IMO seismograms been analysed for SWS before the impending earthquakes (Table 2). | [6, 7, 8, 9] |
| 6) | Extreme sensitivity where stress-accumulation and stress-relaxation were observed in Iceland before the 2004 $M_W$ ~9.2 Sumatra Earthquake at ~10,500 km from Indonesia (Table 3). | [10] |
| 7) | Nearly identical SWS-implied stress-induced behaviour before earthquakes and volcanic eruptions (Figures 7a and 7b; Figures 1 and 2, Paper 1). | [11] |
| 8) | New properties of New Geophysics allow resolution of five earthquake conundrums that are inexplicable in terms of conventional sub-critical geophysics. | [12, 13, 14] |

† References: [1] Crampin (1994); [2] Crampin and Peacock (2008); [3] Crampin and Gao Y (2013); [4] Angerer et al. (2002); [5] Crampin et al. (2003); [6] Crampin et al. (1999); [7] Crampin et al. (2004b); [8] Crampin et al. (2008); [9] Paper 1; [10] Crampin and Gao Y (2012); [11] Liu S et al. (2014); [12] Crampin et al. (2013); [14] this paper.

fracturing at fracture-criticality. Each example cannot be easily explained by conventional sub-critical geophysics. There are no known exceptions where the properties of New Geophysics listed in Table S1 are denied. The importance of this is that critical-systems impose a range of fundamentally-new properties on conventional sub-critical geophysics, as listed in Table S1, that satisfy the criteria for New Geophysics.

Many or most of the properties of New Geophysics in Table S1 are self supporting. If New Geophysics holds, then, for example, P7 Universality suggests that New Geophysics is true in all possible regimes where suitable conditions are present. It seems that SWS in the upper mantle is possibly due to intergranular films of hydrated melt rather than oriented crystals. Similarly P8 Sensitivity provides confidence that changes in SWS in Iceland are monitoring changes caused by stress-accumulation before the 2004, $M$ 9.2, Sumatra earthquake in Indonesia at a distance of 10,500 km in Indonesia.

When the ideas underlying New Geophysics were being initially developed/discovered, one of the most astonishing features was that the range of shear-wave velocity anisotropy was the same everywhere: ~1.5% to ~4.5% in all rocks, from 20% porosity sandstones to 2% porosity metamorphic rocks (Crampin, 1994). This is a feature of Property P3 Uniformity, where similar behaviour is almost universally present. Overall, New Geophysics provides a unifying concept that allows much, otherwise conflicting, seismological behaviour to be united under one all-embracing concept. Many seismological conundrums are resolved properly.

A final comment: It is difficult to recognize when rock is in the critical or the conventional sub-critical state. However, earthquakes provide opportunities to study and compare the New Geophysics critical system and the conventional sub-critical system. To reach a new understanding, more samples and integration from observations are necessary. The authors urge greater attention to New Geophysics on the part of the world's seismologists.

## Acknowledgements

The authors thank: Sheila Peacock and Francesca Bianco for numerous discussions about shear-wave splitting, which greatly improved the manuscript; Brian Baptie, David Booth, Richard Luckett, and the late Russ Evans for valuable comments on the manuscript. Yuan Gao was supported by the Chinese NSFC Project 41474032. We thank the Director of Science and Technology of the British Geological Survey (NERC) for permission to publish this paper. Comments and suggestions of two anonymous reviewers and editors were of valuable assistance in improving this manuscript.

## Supplementary Material

### Brief Summary of New Geophysics

Analysis of worldwide observations of stress-aligned SWS throughout the Earth's crust and upper mantle show that distributions of fluid-saturated stress-aligned vertical microcracks are so closely spaced that they verge on fracture-criticality and fracturing if there is any disturbance (Crampin, 1994; Crampin and Peacock, 2005, 2008). In the uppermost ~400 km of the mantle the 'microcracks' are arguably intergranular films of hydrated melt (Crampin, 2003). Phenomena verging on failure in this way are critical-systems which are part of a *New Physics* (Davies, 1989b), hence the proposed *New Geophysics* reviewed by Crampin and Gao Y (2013). Critical-systems occur in all complex heterogeneous interactive phenomena as they approach singularities (in the case of the Earth, the singularity is at fracture-criticality), where below

criticality the behaviour can be calculated/modelled by standard conventional sub–critical physics (or geophysics). However, at singularities there is deterministic chaos, where the behaviour can still be calculated, but the results may show orders of magnitude differences for minuscule differences in the initial conditions (Lorenz, 1972). Such critical-systems of complex heterogeneous interactive phenomena are very common: the weather; climate change; the life cycle of fruit flies; stellar radiation; the New York stock exchange; etc. (Crampin et al., 2003). Hence, it must be expected that the Earth, an archetypal complex heterogeneous interactive phenomenon, must also be a critical-system with Lorenz-type sensitivity to initial conditions. The criticality of New Geophysics imposes a range of fundamentally-new properties on conventional sub-critical geophysics, some of which are listed in Table S1 (Crampin and Gao Y, 2013). All properties in Table S1 have been observed (with one exception), many times. The exception, P6 Controllability, has not yet been tested. These properties cannot be understood by geoscientists restricted to experience in conventional sub-critical geophysics. A paradigm shift in understanding is required. It is hoped that the potential stress-forecasts plotted in Figures 1 and 2, Paper 1, and the evidence in this paper will promote paradigm shifts in understanding.

**Table S1.** Properties of the New Geophysics of a compliant critically-microcracked Earth (Crampin and Gao Y, 2013)

| | Property | Description | Ref.† |
|---|---|---|---|
| P1) | Self-similarity | Logarithmic plots of many properties are linear, e.g. Gutenberg-Richter relationship. | [1, 2] |
| P2) | Monitorability | Behaviour can be monitored with SWS. | [3, 4, 5] |
| P3) | Uniformity | Statistical behaviour is more like other critical systems than it is to the underlying sub-critical geophysics. | [4, 5] |
| P4) | Calculability | Behaviour is more uniform (universal) than sub-critical behaviour and can be modelled or calculated with the equations of Anisotropic Poro-Elasticity (APE). | [5, 6, 7] |
| P5) | Predictability | If impending changes can be quantified, behaviour can be predicted by APE. | [5, 6, 7] |
| P6) | Controllability | If conditions can be monitored (P2), calculated (P4) and modified by injection pressures (P5), in principle behaviour of *in situ* rock can be controlled by feedback (optimising flow-directions by fluid-injection, say, in hydrocarbon production). | |
| P7) | Universality | Effects pervade all available space. | [8, 9] |
| P8) | Sensitivity | Sensitive to small earthquakes. Sensitive enlargement of little disturbances conforming to tectonics and geophysical conditions, called also "Butterfly-effect" sensitivity to minuscule differences in initial conditions. | [8, 9, 10] |

† References: [1] Gutenberg and Richter (1956); [2] Gao Y and Crampin (2004); [3] Crampin (1999); [4] Crampin and Peacock (2005); [5] Crampin and Peacock (2008); [6] Angerer et al. (2002); [7] Crampin and Zatsepin (1997); [8] Volti and Crampin (2003); [9] Crampin and Gao Y (2012); [10] Lorenz (1972).

## References


Alford, R. M. (1986). Shear data in the presence of azimuthal anisotropy: Dilley, Texas. In *Proceedings of the 56th Ann. Int. Mtg* (pp. 476–379). Houston: SEG. https://doi.org/10.1190/1.1893036

Allmann, B. P., and Shearer, P. M. (2009). Global variations of stress drop for moderate to large earthquakes. *J. Geophys. Res.*, *114*(B1), B01310. https://doi.org/10.1029/2008JB005821

Angerer, E., Crampin, S., Li, X. Y., and Davis, T. L. (2002). Processing, modelling and predicting time-lapse effects of overpressured fluid-injection in a fractured reservoir. *Geophys. J. Int.*, *149*(2), 267–280. https://doi.org/10.1046/j.1365-246X.2002.01607.x

Bak, P. (1996). *How Nature Works: the Science of Self-Organized Criticality*. New York: Springer-Verlag.

Baltay, A., Ide, S., Prieto, G., and Beroza, G. (2011). Variability in earthquake stress drop and apparent stress. *Geophys. Res. Lett.*, *38*(6), L06303. https://doi.org/10.1029/2011GL046698

Booth, D. C., and Crampin, S. (1985). Shear-wave polarizations on a curved wavefront at an isotropic free-surface. *Geophys. J. R. Astron. Soc.*, *83*, 31–45.

Booth, D. C., Crampin, S., Lovell, J. H., and Chiu, J. M. (1990). Temporal changes in shear wave splitting during an earthquake swarm in Arkansas. *J. Geophys. Res.*, *95*(B7), 11151–11164. https://doi.org/10.1029/JB095iB07p11151

Crampin, S. (1970). The dispersion of surface waves in multilayered anisotropic media. *Geophys. J. R. Astron. Soc.*, *21*(3), 387–402. https://doi.org/10.1111/j.1365-246X.1970.tb01799.x

Crampin, S., and King, D. W. (1977). Evidence for anisotropy in the upper mantle beneath Eurasia from the polarization of higher mode seismic surface waves. *Geophys. J. R. Astron. Soc.*, *49*(1), 59–85. https://doi.org/10.1111/j.1365-246X.1977.tb03701.x

Crampin, S. (1981). A review of wave motion in anisotropic and cracked elastic-media. *Wave Motion*, *3*(4), 343–391. https://doi.org/10.1016/0165-2125(81)90026-3

Crampin, S., and Kirkwood, S. C. (1981). Velocity variations in systems of anisotropic symmetry. *J. Geophys.*, *49*, 35–42.

Crampin, S., Booth, D. C., Evans, R., Peacock, S., and Fletcher, J. B. (1990). Changes in shear wave splitting at Anza near the time of the North Palm Springs Earthquake. *J. Geophys. Res.*, *95*(B7), 11197–11212. https://doi.org/10.1029/JB095iB07p11197

Crampin, S., Booth, D. C., Evans, R., Peacock, S., and Fletcher, J. B. (1991). Comment on "Quantitative measurements of shear wave polarizations at the anza seismic network, Southern California: implications for shear wave splitting and earthquake prediction" by Richard C. Aster, Peter M. Shearer, and Jon Berger. *J. Geophys. Res.*, *96*(B4), 6403–6414. https://doi.org/10.1029/90JB02453

Crampin, S. (1994). The fracture criticality of crustal rocks. *Geophys. J. Int.*, *118*(2), 428–438. https://doi.org/10.1111/j.1365-246X.1994.tb03974.x

Crampin, S., Zatsepin, S. V., Slater, C., and Brodov, L. Y. (1996). Abnormal shear wave polarizations as indicators of high pressures and over pressures. In *Proceedings of the 58th Conference European Association of Geophysicists and Engineers*. Amsterdam: EAGE.

Crampin, S., and Zatsepin, S. V. (1997). Modelling the compliance of crustal rock-Ⅱ. Response to temporal changes before earthquakes. *Geophys. J. Int.*, *129*(3), 495–506. https://doi.org/10.1111/j.1365-246X.1997.tb04489.x

Crampin, S. (1999). Calculable fluid-rock interactions. *J. Geol. Soc.*, *156*(3),

501–514. https://doi.org/10.1144/gsjgs.156.3.0501
Crampin, S., Volti, T., and Stefánsson, R. (1999). A successfully stress-forecast earthquake. *Geophys. J. Int.*, *138*, F1–F5.
Crampin, S., Volti, T., Chastin, S., Gudmundsson, A., and Stefánsson, R. (2002). Indication of high pore-fluid pressures in a seismically-active fault zone. *Geophys. J. Int.*, *151*(2), F1–F5. https://doi.org/10.1046/j.1365-246X.2002.01830.x
Crampin, S. (2003). Aligned cracks not LPO as the cause of mantle anisotropy. In *EGS-AGU-EUG Joint Assembly*, Nice. Nice, France: AGU.
Crampin, S., Chastin, S., and Gao, Y. (2003). Shear-wave splitting in a critical crust: III. Preliminary report of multi-variable measurements in active tectonics. *J. Appl. Geophys.*, *54*(3-4), 265–277. https://doi.org/10.1016/j.jappgeo.2003.01.001
Crampin, S. (2004). The New Geophysics: implications for hydrocarbon recovery and possible contamination of time-lapse seismics. *First Break*, *22*(6), 73–82. https://doi.org/10.3997/1365-2397.2004010
Crampin, S., Peacock, S., Gao, Y., and Chastin. S. (2004a). The scatter of time-delays in shear-wave splitting above small earthquakes. *Geophys. J. Int.*, *156*(1), 39–44. https://doi.org/10.1111/j.1365-246X.2004.02040.x
Crampin, S., Volti, T., and Stefánsson, R. (2004b). Response to 'A statistical evaluation of a 'stress-forecast' earthquake' by T. Seher & I. G. Main. *Geophys. J. Int.*, *157*(1), 194–199. https://doi.org/10.1111/j.1365-246X.2004.02187.x
Crampin, S., and Gao, Y. (2005). Comment on "Systematic analysis of shear-wave splitting in the aftershock zone of the 1999 Chi-Chi, Taiwan, earthquake: shallow crustal anisotropy and lack of precursory changes, by Yungfeng Liu, Ta-Liang Teng, and Yehuda Ben-Zion". *Bull. Seismol. Soc. Am.*, *95*(1), 354–360. https://doi.org/10.1785/0120040092
Crampin, S., and Peacock, S. (2005). A review of shear-wave splitting in the compliant crack-critical anisotropic Earth. *Wave Motion*, *41*(1), 59–77. https://doi.org/10.1016/j.wavemoti.2004.05.006
Crampin, S. (2006). The New Geophysics: a new understanding of fluid-rock deformation. In Van Cotthem, A., et al. (Eds.), *Eurock 2006: Multiphysics Coupling and Long Term Behaviour in Rock Mechanics* (pp. 539–544). London: Taylor and Francis.
Crampin, S., and Peacock, S. (2008). A review of the current understanding of seismic shear-wave splitting in the Earth's crust and common fallacies in interpretation. *Wave Motion*, *45*(6), 675–722. https://doi.org/10.1016/j.wavemoti.2008.01.003
Crampin, S., Gao, Y., and Peacock, S. (2008). Stress-forecasting (not predicting) earthquakes: A paradigm shift?. *Geology*, *36*(5), 427–430. https://doi.org/10.1130/G24643A.1
Crampin, S. (2011). A second opinion on "Operational earthquake forecasting: some thoughts on why and how," by Thomas H. Jordan and Lucile M. Jones. Seismol.. *Res. Lett.*, *82*(2), 227–230. https://doi.org/10.1785/gssrl.82.2.227
Crampin, S. (2012). Misunderstandings in comments and replies about the ICEF Report.
Crampin, S., and Gao, Y. (2012). Plate-wide deformation before the Sumatra-Andaman Earthquake. *J. Asian Earth Sci.*, *46*, 61–69. https://doi.org/10.1016/j.jseaes.2011.10.015
Crampin, S., and Gao, Y. (2013). The new geophysics. *Terra Nova*, *25*(3), 173–180. https://doi.org/10.1111/ter.12030
Crampin, S., Gao, Y., and De Santis, A. (2013). A few earthquake conundrums resolved. *J. Asian Earth Sci.*, *62*, 501–509. https://doi.org/10.1016/j.jseaes.2012.10.036
Crampin, S., and Gao, Y. (2015). The physics underlying Gutenberg-Richter in the Earth and in the Moon. *J. Earth Sci.*, *26*(1), 134–139. https://doi.org/10.1007/s12583-015-0513-3
Crampin, S., Gao, Y., and Bukits, J. (2015). A review of retrospective stress-forecasts of earthquakes and eruptions. *Phys. Earth Planet. Inter.*, *245*, 76–87. https://doi.org/10.1016/j.pepi.2015.05.008
Davies, P. (1989a). The new physics: a synthesis. In Davies, P. (Ed.), *The New Physics* (pp. 1–6). Cambridge: Cambridge University Press.
Davies, P. (1989b). *The New Physics*. Cambridge: Cambridge University Press.
Gao, Y., Zheng, S. H., and Sun, Y. (1995). Crack-induced anisotropy in the crust from shear wave splitting observed in Tangshan region, North China. *Acta Seismol. Sinica*, *8*(3), 351–363. https://doi.org/10.1007/BF02650563
Gao, Y. Wang, P. D., Zheng, S. H., Wang, M., Chen, Y. T., and Zhou, H. L. (1998). Temporal changes in shear-wave splitting at an isolated swarm of small earthquakes in 1992 near Dongfang, Hainan Island, Southern China. *Geophys. J. Int.*, *135*(1), 102–112. https://doi.org/10.1046/j.1365-246X.1998.00606.x
Gao, Y., and Crampin, S. (2003). Temporal variations of shear-wave splitting in field and laboratory studies in China. *J. Appl. Geophys.*, *54*(3-4), 279–287. https://doi.org/10.1016/j.jappgeo.2003.01.002
Gao, Y., and Crampin, S. (2004). Observations of stress relaxation before earthquakes. *Geophys. J. Int.*, *157*(2), 578–582. https://doi.org/10.1111/j.1365-246X.2004.02207.x
Gao, Y., and Crampin, S. (2006). A stress-forecast earthquake (with hindsight), where migration of source earthquakes causes anomalies in shear-wave polarisations. *Tectonophysics*, *426*(3-4), 253–262. https://doi.org/10.1016/j.tecto.2006.07.013
Gao, Y., and Crampin, S. (2008). Shear-wave splitting and earthquake forecasting. *Terra Nova*, *20*(6), 440–448. https://doi.org/10.1111/j.1365-3121.2008.00836.x
Gao, Y., Wu, J., Yi, G. X., and Shi, Y. T. (2010). Crust-mantle coupling in North China: preliminary analysis from seismic anisotropy. *Chin. Sci. Bull.*, *55*(31), 3599–3605. https://doi.org/10.1007/s11434-010-4135-y
Gao, Y., Wu, J., Fukao, Y., Shi, Y. T., and Zhu, A. L. (2011). Shear wave splitting in the crust in North China: stress, faults and tectonic implications. *Geophys. J. Int.*, *187*(2), 642–654. https://doi.org/10.1111/j.1365-246X.2011.05200.x
Geller, R. J. (1997). Earthquake Prediction: a critical review. *Geophys. J. Int.*, *131*(3), 425–450. https://doi.org/10.1111/j.1365-246X.1997.tb06588.x
Geller, R. J., Jackson, D. D., Kagan, Y. Y., Mulargia, F. (1997). Earthquakes cannot be predicted. *Science*, *275*(5306), 1616–1617. https://doi.org/10.1126/science.275.5306.1616
Gerst, A., and Savage, M. K. (2004). Seismic anisotropy beneath Ruapehu volcano: a possible eruption forecasting tool. *Science*, *306*(5701), 1543–1547. https://doi.org/10.1126/science.1103445
Gudmundsson, M. T., Hoskuldsson, A., Larsen, G., Thordarson, T., Oddsson, B., Hognadottir, T., Jonsdottir, I., Bjornsson, H., Petersen, N. G., and Magnusson, E. (2011). Eyjafjallajökull April-June 2010: An explosive-mixed eruption of unusually long duration. In *EGU General Assembly*. Vienna, Austria: EGU.
Gutenberg, B., and Richter, C. F. (1956). Magnitude and energy of earthquakes. *Ann. Geofis.*, *9*, 1–15.
Helbig, K., and Thomsen, L. (2005). 75-plus years of anisotropy in exploration and reservoir seismics: A historical review of concepts and methods. *Geophysics*, *70*(6), 9ND–23ND. https://doi.org/10.1190/1.2122407
Hudson, J. A. (1981). Wave speeds and attenuation of elastic waves in material containing cracks. *Geophys. J. R. Astron. Soc.*, *64*(1), 133–150. https://doi.org/10.1111/j.1365-246X.1981.tb02662.x
Jensen H. J. (1998). *Self-Organized Criticality*. Cambridge: Cambridge University Press.
Jordan, T. H., and Jones, L. M. (2011). Reply to 'A second opinion on "Operational earthquake forecasting: some thoughts on why and how," by Thomas H. Jordan and Lucile M. Jones,' by Stuart Crampin. *Seismol. Res. Lett.*, *82*(2), 231–232. https://doi.org/10.1785/gssrl.82.2.231
Jordan, T. H., Chen, Y. T., Gasparini, P., Madariaga, R., Main, I., Marzocchi, W., Papadopoulos, G., Sobolev, G., Yamaoka, K., and Zschau, J. (2012). Reply to "Comment on 'Operational earthquake forecasting: Status of knowledge and guidelines for implementation by Jordan et al. [2011]' by Stuart Crampin". *Ann. Geophys.*, *55*(1), 13–15. https://doi.org/10.4401/ag-5690
Kossobokov, V. G. (2013). Earthquake prediction: 20 years of global experiment. *Nat. Haz.*, *69*(2), 1157–1177. https://doi.org/10.1007/s11069-012-0198-1
Leary, P. (1991). Deep borehole log evidence for fractal distribution of fractures in crystalline rock. *Geophys. J. Int.*, *107*(3), 615–627. https://doi.org/10.1111/j.1365-246X.1991.tb01421.x
Liu, S., Crampin, S., Luckett, R., and Yang, J. S. (2014). Changes in shear wave splitting before the 2010 Eyjafjallajökull eruption in Iceland. *Geophys. J. Int.*, *199*(1), 102–112. https://doi.org/10.1093/gji/ggu202
Liu, Y., Crampin, S., and Main, I. (1997). Shear-wave anisotropy: spatial and temporal variations in time delays at Parkfield, Central California. *Geophys. J.*

*Int.*, *130*(3), 771–785. https://doi.org/10.1111/j.1365-246X.1997.tb01872.x

Lorenz, E. N. (1972). Predictability: does the flap of a butterfly's wings in Brazil set off a tornado in Texas?. In *Proceedings of the 139th Annual Meeting of the American Association for the Advancement of Science*. Cambridge: Massachusetts Institute of Technology.

Peacock, S., Crampin, S., Booth, D. C., and Fletcher, J. B. (1988). Shear wave splitting in the Anza seismic gap, Southern California: temporal variations as possible precursors. *J. Geophys. Res.*, *93*(B4), 3339–3356. https://doi.org/10.1029/JB093iB04p03339

Roche, S. L., Davis, T. L., and Benson, R. D. (1997). 4-D, 3-C seismic study at Vacuum field, New Mexico. In *1997 SEG Annual Meeting* (pp. 886–889). Dallas, Texas: SEG.

Savage, H. M., and Brodsky, E. E. (2011). Collateral damage: evolution with displacement of fracture distribution and secondary fault strands in fault damage zones. *J. Geophys. Res.*, *116*(B3), B03405. https://doi.org/10.1029/2010JB007665

Savage, M. K. (1999). Seismic anisotropy and mantle deformation: What have we learned from shear wave splitting?. *Rev. Geophys.*, *37*(1), 65–106. https://doi.org/10.1029/98RG02075

Shao, Y. P., Gao, Y., Dai, S. G., Du, Y., and Song, C. (2017). Seismic shear-wave splitting characteristics in the crust in the area of Jinping reservoir of Sichuan and influences from water impoundment. *Chin. J. Geophys.*, *60*(12), 4557–4568. https://doi.org/10.6038/cjg20171203

Shi, Y. T., Gao, Y., Zhao, C. P., Yao, Z. X., and Zhang, Y. J. (2009). A study of seismic anisotropy of Wenchuan earthquake sequence. *Chin. J. Geophys.*, *52*(1), 138–147. https://doi.org/10.1002/cjg2.1335

Silver, P. G. (1996). Seismic anisotropy beneath the continents: probing the depths of geology. *Ann. Rev. Earth Planet. Sci.*, *24*, 385–432. https://doi.org/10.1146/annurev.earth.24.1.385

Tai, L. X., Gao, Y., Cao, F. J., Wu, J., Shi, Y. T., and Jiao, M. R. (2008). Shear-wave splitting beforeand after the 1999 Xiuyan earthquake in Liaoning, China. *Acta Seismol. Sinica*, *21*(4), 344–357. https://doi.org/10.1007/s11589-008-0344-8

Teanby, N. A., Kendall, J. M., Jones, R. H., and Barkved, O. (2004). Stress-induced temporal variations in seismic anisotropy observed in microseismic data. *Geophys. J. Int.*, *156*(3), 459–466. https://doi.org/10.1111/j.1365-246X.2004.02212.x

Volti, T., and Crampin, S. (2003). A four-year study of shear-wave splitting in Iceland: 2. Temporal changes before earthquakes and volcanic eruptions. In Nieuwland, D. A. (Ed.), *New Insights into Structural Interpretation and Modelling* (pp. 135–149). Geological Society, London, Special Publication.

Walter, L. A., Leary, P. C., and Crampin, S. (2003). Physical model for downhole orbital vibrator (DOV) – (2) borehole seismic radiation. In *Proceedings of the 73rd Ann. Int. Mtg* (pp. 1536–1539). Dallas, Texas: SEG. https://doi.org/10.1190/1.1817795

Wu, J., Crampin, S., Gao, Y., Hao, P., Volti, T., and Chen, Y. T. (2006). Smaller source earthquakes and improved measuring techniques allow the largest earthquakes in Iceland to be stress forecast (with hindsight). *Geophys. J. Int.*, *166*(3), 1293–1298. https://doi.org/10.1111/j.1365-246X.2006.03054.x

Zatsepin, S. V., and Crampin, S. (1997). Modelling the compliance of crustal rock-I. Response of shear-wave splitting to differential stress. *Geophys. J. Int.*, *129*(3), 477–494. https://doi.org/10.1111/j.1365-246X.1997.tb04488.x

Zhao, B., Shi, Y. T., and Gao, Y. (2012). Seismic relocation, focal mechanism and crustal seismic anisotropy associated with the 2010 Yushu $M_S$7.1 earthquake and its aftershocks.. *Earthq. Sci.*, *25*(1), 111–119. https://doi.org/10.1007/s11589-012-0837-3